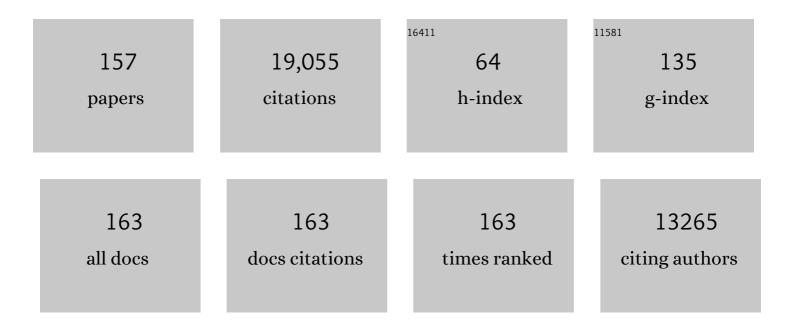
Sebastien Boutet

List of Publications by Year in descending order

Source: https://exaly.com/author-pdf/9061589/publications.pdf Version: 2024-02-01



#	Article	IF	CITATIONS
1	Observations of phase changes in monoolein during high viscous injection. Journal of Synchrotron Radiation, 2022, 29, 602-614.	1.0	5
2	Ultrafast structural changes within a photosynthetic reaction centre. Nature, 2021, 589, 310-314.	13.7	47
3	Observation of shock-induced protein crystal damage during megahertz serial femtosecond crystallography. Physical Review Research, 2021, 3, .	1.3	8
4	Synchronous RNA conformational changes trigger ordered phase transitions in crystals. Nature Communications, 2021, 12, 1762.	5.8	17
5	Early-stage dynamics of chloride ion–pumping rhodopsin revealed by a femtosecond X-ray laser. Proceedings of the National Academy of Sciences of the United States of America, 2021, 118, .	3.3	41
6	Effect of X-ray free-electron laser-induced shockwaves on haemoglobin microcrystals delivered in a liquid jet. Nature Communications, 2021, 12, 1672.	5.8	21
7	Mechanism and dynamics of fatty acid photodecarboxylase. Science, 2021, 372, .	6.0	93
8	Ultrafast X-ray scattering offers a structural view of excited-state charge transfer. Proceedings of the United States of America, 2021, 118, .	3.3	18
9	Serial crystallography using automated drop dispensing. Journal of Synchrotron Radiation, 2021, 28, 1386-1392.	1.0	1
10	Femtosecond quantification of void evolution during rapid material failure. Science Advances, 2020, 6, .	4.7	22
11	Structural dynamics in proteins induced by and probed with X-ray free-electron laser pulses. Nature Communications, 2020, 11, 1814.	5.8	57
12	Serial femtosecond crystallography on in vivo-grown crystals drives elucidation of mosquitocidal Cyt1Aa bioactivation cascade. Nature Communications, 2020, 11, 1153.	5.8	31
13	X-ray diffractive imaging of controlled gas-phase molecules: Toward imaging of dynamics in the molecular frame. Journal of Chemical Physics, 2020, 152, 084307.	1.2	24
14	Observation of the molecular response to light upon photoexcitation. Nature Communications, 2020, 11, 2157.	5.8	42
15	Advances in ultrafast gas-phase x-ray scattering. Journal of Physics B: Atomic, Molecular and Optical Physics, 2020, 53, 234004.	0.6	20
16	The ePix10k 2-megapixel hard X-ray detector at LCLS. Journal of Synchrotron Radiation, 2020, 27, 608-615.	1.0	24
17	Comparing serial X-ray crystallography and microcrystal electron diffraction (MicroED) as methods for routine structure determination from small macromolecular crystals. IUCrJ, 2020, 7, 306-323.	1.0	32
18	Harnessing the power of an X-ray laser for serial crystallography of membrane proteins crystallized in lipidic cubic phase. IUCrJ, 2020, 7, 976-984.	1.0	15

#	Article	IF	CITATIONS
19	Double grating shearing interferometry for X-ray free-electron laser beams. Optica, 2020, 7, 404.	4.8	9
20	Three-dimensional view of ultrafast dynamics in photoexcited bacteriorhodopsin. Nature Communications, 2019, 10, 3177.	5.8	121
21	Ultrafast X-ray scattering reveals vibrational coherence following Rydberg excitation. Nature Chemistry, 2019, 11, 716-721.	6.6	73
22	Coherent diffractive imaging of microtubules using an X-ray laser. Nature Communications, 2019, 10, 2589.	5.8	22
23	A deep UV trigger for ground-state ring-opening dynamics of 1,3-cyclohexadiene. Science Advances, 2019, 5, eaax6625.	4.7	35
24	Scattering off molecules far from equilibrium. Journal of Chemical Physics, 2019, 151, 084301.	1.2	16
25	Performance of ePix10K, a high dynamic range, gain auto-ranging pixel detector for FELs. AIP Conference Proceedings, 2019, , .	0.3	11
26	Simplicity Beneath Complexity: Counting Molecular Electrons Reveals Transients and Kinetics of Photodissociation Reactions. Angewandte Chemie - International Edition, 2019, 58, 6371-6375.	7.2	25
27	Snapshot of an oxygen intermediate in the catalytic reaction of cytochrome <i>c</i> oxidase. Proceedings of the National Academy of Sciences of the United States of America, 2019, 116, 3572-3577.	3.3	70
28	X-ray Emission Spectroscopy at X-ray Free Electron Lasers: Limits to Observation of the Classical Spectroscopic Response for Electronic Structure Analysis. Journal of Physical Chemistry Letters, 2019, 10, 441-446.	2.1	8
29	Generation of high-intensity ultrasound through shock propagation in liquid jets. Physical Review Fluids, 2019, 4, .	1.0	11
30	3D printed droplet generation devices for serial femtosecond crystallography enabled by surface coating. Journal of Applied Crystallography, 2019, 52, 997-1008.	1.9	19
31	The Macromolecular Femtosecond Crystallography Instrument at the Linac Coherent Light Source. Journal of Synchrotron Radiation, 2019, 26, 346-357.	1.0	37
32	Nanofocus characterization at the Coherent X-ray Imaging instrument using 2D single grating interferometry. , 2019, , .		2
33	Structure-factor amplitude reconstruction from serial femtosecond crystallography of two-dimensional membrane-protein crystals. IUCrJ, 2019, 6, 34-45.	1.0	1
34	Stimulated X-Ray Emission Spectroscopy in Transition Metal Complexes. Physical Review Letters, 2018, 120, 133203.	2.9	48
35	Chromophore twisting in the excited state of a photoswitchable fluorescent protein captured by time-resolved serial femtosecond crystallography. Nature Chemistry, 2018, 10, 31-37.	6.6	152
36	A statistical approach to detect protein complexes at X-ray freeÂelectron laser facilities. Communications Physics, 2018, 1, .	2.0	2

#	Article	IF	CITATIONS
37	Determining Orientations of Optical Transition Dipole Moments Using Ultrafast X-ray Scattering. Journal of Physical Chemistry Letters, 2018, 9, 6556-6562.	2.1	36
38	Structures of the intermediates of Kok's photosynthetic water oxidation clock. Nature, 2018, 563, 421-425.	13.7	386
39	Relativistic and resonant effects in the ionization of heavy atoms by ultra-intense hard X-rays. Nature Communications, 2018, 9, 4200.	5.8	29
40	Ultrafast nonthermal heating of water initiated by an X-ray Free-Electron Laser. Proceedings of the National Academy of Sciences of the United States of America, 2018, 115, 5652-5657.	3.3	28
41	Femtosecond X-ray coherent diffraction of aligned amyloid fibrils on low background graphene. Nature Communications, 2018, 9, 1836.	5.8	34
42	High-accuracy wavefront sensing for x-ray free electron lasers. Optica, 2018, 5, 967.	4.8	53
43	X-Ray Free Electron Lasers and Their Applications. , 2018, , 1-21.		8
44	Resolution extension by image summing in serial femtosecond crystallography of two-dimensional membrane-protein crystals. IUCrJ, 2018, 5, 103-117.	1.0	8
45	Atomic structure of granulin determined from native nanocrystalline granulovirus using an X-ray free-electron laser. Proceedings of the National Academy of Sciences of the United States of America, 2017, 114, 2247-2252.	3.3	65
46	Diffraction data of core-shell nanoparticles from an X-ray free electron laser. Scientific Data, 2017, 4, 170048.	2.4	4
47	Flowâ€aligned, singleâ€shot fiber diffraction using a femtosecond Xâ€ray freeâ€electron laser. Cytoskeleton, 2017, 74, 472-481.	1.0	12
48	Femtosecond response of polyatomic molecules to ultra-intense hard X-rays. Nature, 2017, 546, 129-132.	13.7	139
49	Double-flow focused liquid injector for efficient serial femtosecond crystallography. Scientific Reports, 2017, 7, 44628.	1.6	90
50	Focal Spot and Wavefront Sensing of an X-Ray Free Electron laser using Ronchi shearing interferometry. Scientific Reports, 2017, 7, 13698.	1.6	19
51	Se-SAD serial femtosecond crystallography datasets from selenobiotinyl-streptavidin. Scientific Data, 2017, 4, 170055.	2.4	6
52	How Cubic Can Ice Be?. Journal of Physical Chemistry Letters, 2017, 8, 3216-3222.	2.1	46
53	Structures of riboswitch RNA reaction states by mix-and-inject XFEL serial crystallography. Nature, 2017, 541, 242-246.	13.7	251
54	Measurements of Long-range Electronic Correlations During Femtosecond Diffraction Experiments Performed on Nanocrystals of Buckminsterfullerene. Journal of Visualized Experiments, 2017, , .	0.2	3

#	Article	IF	CITATIONS
55	X-ray Free Electron Laser Determination of Crystal Structures of Dark and Light States of a Reversibly Photoswitching Fluorescent Protein at Room Temperature. International Journal of Molecular Sciences, 2017, 18, 1918.	1.8	14
56	Nanocrystallography measurements of early stage synthetic malaria pigment. Journal of Applied Crystallography, 2017, 50, 1533-1540.	1.9	11
57	Numerical simulations of the hard X-ray pulse intensity distribution at the Linac Coherent Light Source. Journal of Synchrotron Radiation, 2017, 24, 738-743.	1.0	6
58	Experimental strategies for imaging bioparticles with femtosecond hard X-ray pulses. IUCrJ, 2017, 4, 251-262.	1.0	63
59	Analysis of XFEL serial diffraction data from individual crystalline fibrils. IUCrJ, 2017, 4, 795-811.	1.0	16
60	Protein structure determination by single-wavelength anomalous diffraction phasing of X-ray free-electron laser data. IUCrJ, 2016, 3, 180-191.	1.0	71
61	Establishing nonlinearity thresholds with ultraintense X-ray pulses. Scientific Reports, 2016, 6, 33292.	1.6	43
62	Selenium single-wavelength anomalous diffraction de novo phasing using an X-ray-free electron laser. Nature Communications, 2016, 7, 13388.	5.8	40
63	X-ray laser–induced electron dynamics observed by femtosecond diffraction from nanocrystals of Buckminsterfullerene. Science Advances, 2016, 2, e1601186.	4.7	20
64	Coherent diffraction of single Rice Dwarf virus particles using hard X-rays at the Linac Coherent Light Source. Scientific Data, 2016, 3, 160064.	2.4	64
65	Lipidic cubic phase injector is a viable crystal delivery system for time-resolved serial crystallography. Nature Communications, 2016, 7, 12314.	5.8	71
66	Negative Pressures and Spallation in Water Drops Subjected to Nanosecond Shock Waves. Journal of Physical Chemistry Letters, 2016, 7, 2055-2062.	2.1	40
67	Liquid explosions induced by X-ray laser pulses. Nature Physics, 2016, 12, 966-971.	6.5	116
68	Femtosecond structural dynamics drives the trans/cis isomerization in photoactive yellow protein. Science, 2016, 352, 725-729.	6.0	348
69	De novo phasing with X-ray laser reveals mosquito larvicide BinAB structure. Nature, 2016, 539, 43-47.	13.7	98
70	Structure of photosystem II and substrate binding at room temperature. Nature, 2016, 540, 453-457.	13.7	323
71	Linac Coherent Light Source: The first five years. Reviews of Modern Physics, 2016, 88, .	16.4	477
72	Native phasing of x-ray free-electron laser data for a G protein–coupled receptor. Science Advances, 2016. 2. e1600292.	4.7	97

#	Article	IF	CITATIONS
73	The room temperature crystal structure of a bacterial phytochrome determined by serial femtosecond crystallography. Scientific Reports, 2016, 6, 35279.	1.6	39
74	X-ray laser diffraction for structure determination of the rhodopsin-arrestin complex. Scientific Data, 2016, 3, 160021.	2.4	51
75	Serial femtosecond crystallography datasets from G protein-coupled receptors. Scientific Data, 2016, 3, 160057.	2.4	10
76	The New Macromolecular Femtosecond Crystallography (MFX) Instrument at LCLS. Synchrotron Radiation News, 2016, 29, 23-28.	0.2	31
77	Macromolecular diffractive imaging using imperfect crystals. Nature, 2016, 530, 202-206.	13.7	123
78	Transient lattice contraction in the solid-to-plasma transition. Science Advances, 2016, 2, e1500837.	4.7	70
79	Concentric-flow electrokinetic injector enables serial crystallography of ribosome and photosystem II. Nature Methods, 2016, 13, 59-62.	9.0	103
80	A novel inert crystal delivery medium for serial femtosecond crystallography. IUCrJ, 2015, 2, 421-430.	1.0	123
81	Towards phasing using high X-ray intensity. IUCrJ, 2015, 2, 627-634.	1.0	24
82	Serial femtosecond crystallography of soluble proteins in lipidic cubic phase. IUCrJ, 2015, 2, 545-551.	1.0	61
83	Serial femtosecond X-ray diffraction of enveloped virus microcrystals. Structural Dynamics, 2015, 2, 041720.	0.9	11
84	Strongly aligned gas-phase molecules at free-electron lasers. Journal of Physics B: Atomic, Molecular and Optical Physics, 2015, 48, 204002.	0.6	28
85	Using Ultrafast X-ray Lasers to Image Structure & Dynamics. Microscopy and Microanalysis, 2015, 21, 1849-1850.	0.2	0
86	Trace phase detection and strain characterization from serial X-ray free-electron laser crystallography of a Pr _{0.5} Ca _{0.5} MnO ₃ powder. Powder Diffraction, 2015, 30, S25-S30.	0.4	1
87	Ternary structure reveals mechanism of a membrane diacylglycerol kinase. Nature Communications, 2015, 6, 10140.	5.8	30
88	Structural basis for bifunctional peptide recognition at human δ-opioid receptor. Nature Structural and Molecular Biology, 2015, 22, 265-268.	3.6	151
89	Indications of radiation damage in ferredoxin microcrystals using high-intensity X-FEL beams. Journal of Synchrotron Radiation, 2015, 22, 225-238.	1.0	110
90	Characterization and use of the spent beam for serial operation of LCLS. Journal of Synchrotron Radiation, 2015, 22, 634-643.	1.0	17

#	Article	IF	CITATIONS
91	Effects of self-seeding and crystal post-selection on the quality of Monte Carlo-integrated SFX data. Journal of Synchrotron Radiation, 2015, 22, 644-652.	1.0	20
92	Optical laser systems at the Linac Coherent Light Source. Journal of Synchrotron Radiation, 2015, 22, 526-531.	1.0	42
93	Demonstration of simultaneous experiments usingÂthin crystal multiplexing at the Linac CoherentÂLight Source. Journal of Synchrotron Radiation, 2015, 22, 626-633.	1.0	20
94	Anomalous Behavior of the Homogeneous Ice Nucleation Rate in "No-Man's Land― Journal of Physical Chemistry Letters, 2015, 6, 2826-2832.	2.1	102
95	Crystal structure of rhodopsin bound to arrestin by femtosecond X-ray laser. Nature, 2015, 523, 561-567.	13.7	683
96	Structure of the Angiotensin Receptor Revealed by Serial Femtosecond Crystallography. Cell, 2015, 161, 833-844.	13.5	315
97	The Coherent X-ray Imaging instrument at the Linac Coherent Light Source. Journal of Synchrotron Radiation, 2015, 22, 514-519.	1.0	152
98	Toxicity of Eosinophil MBP Is Repressed by Intracellular Crystallization and Promoted by Extracellular Aggregation. Molecular Cell, 2015, 57, 1011-1021.	4.5	88
99	Anomalous nonlinear X-ray Compton scattering. Nature Physics, 2015, 11, 964-970.	6.5	99
100	Direct observation of ultrafast collective motions in CO myoglobin upon ligand dissociation. Science, 2015, 350, 445-450.	6.0	344
101	Structure of the toxic core of α-synuclein from invisible crystals. Nature, 2015, 525, 486-490.	13.7	528
102	Low-Zpolymer sample supports for fixed-target serial femtosecond X-ray crystallography. Journal of Applied Crystallography, 2015, 48, 1072-1079.	1.9	32
103	Structural studies of P-type ATPase–ligand complexes using an X-ray free-electron laser. IUCrJ, 2015, 2, 409-420.	1.0	20
104	Experience with the CSPAD during dedicated detector runs at LCLS. Journal of Physics: Conference Series, 2014, 493, 012011.	0.3	15
105	Femtosecond X-ray diffraction from two-dimensional protein crystals. IUCrJ, 2014, 1, 95-100.	1.0	78
106	Expression, purification and crystallization of CTB-MPR, a candidate mucosal vaccine component against HIV-1. IUCrJ, 2014, 1, 305-317.	1.0	6
107	Performance of a beam-multiplexing diamond crystal monochromator at the Linac Coherent Light Source. Review of Scientific Instruments, 2014, 85, 063106.	0.6	55
108	Time-resolved serial crystallography captures high-resolution intermediates of photoactive yellow protein. Science, 2014, 346, 1242-1246.	6.0	418

#	Article	IF	CITATIONS
109	Silicon Mirrors for High-Intensity X-Ray Pump and Probe Experiments. Physical Review Applied, 2014, 1, .	1.5	6
110	Lipidic cubic phase injector facilitates membrane protein serial femtosecond crystallography. Nature Communications, 2014, 5, 3309.	5.8	505
111	Accurate macromolecular structures using minimal measurements from X-ray free-electron lasers. Nature Methods, 2014, 11, 545-548.	9.0	140
112	Tracking excited-state charge and spin dynamics in iron coordination complexes. Nature, 2014, 509, 345-348.	13.7	382
113	De novo protein crystal structure determination from X-ray free-electron laser data. Nature, 2014, 505, 244-247.	13.7	245
114	7 Ã resolution in protein two-dimensional-crystal X-ray diffraction at Linac Coherent Light Source. Philosophical Transactions of the Royal Society B: Biological Sciences, 2014, 369, 20130500.	1.8	32
115	Visualizing a protein quake with time-resolved X-ray scattering at a free-electron laser. Nature Methods, 2014, 11, 923-926.	9.0	173
116	Protein crystal structure obtained at 2.9 Ã resolution from injecting bacterial cells into an X-ray free-electron laser beam. Proceedings of the National Academy of Sciences of the United States of America, 2014, 111, 12769-12774.	3.3	111
117	Ultrafast X-ray probing of water structure below the homogeneous ice nucleation temperature. Nature, 2014, 510, 381-384.	13.7	385
118	Serial time-resolved crystallography of photosystem II using a femtosecond X-ray laser. Nature, 2014, 513, 261-265.	13.7	403
119	Taking snapshots of photosynthetic water oxidation using femtosecond X-ray diffraction and spectroscopy. Nature Communications, 2014, 5, 4371.	5.8	206
120	Silicon single crystal as back-reflector for high-intensity hard x-rays. , 2014, , .		0
121	Fixed-target protein serial microcrystallography with an x-ray free electron laser. Scientific Reports, 2014, 4, 6026.	1.6	169
122	Serial femtosecond X-ray diffraction of 30S ribosomal subunit microcrystals in liquid suspension at ambient temperature using an X-ray free-electron laser. Acta Crystallographica Section F: Structural Biology Communications, 2013, 69, 1066-1069.	0.7	32
123	Serial Femtosecond Crystallography of G Protein–Coupled Receptors. Science, 2013, 342, 1521-1524.	6.0	424
124	Structure of a photosynthetic reaction centre determined by serial femtosecond crystallography. Nature Communications, 2013, 4, 2911.	5.8	74
125	Natively Inhibited <i>Trypanosoma brucei</i> Cathepsin B Structure Determined by Using an X-ray Laser. Science, 2013, 339, 227-230.	6.0	393
126	Simultaneous Femtosecond X-ray Spectroscopy and Diffraction of Photosystem II at Room Temperature. Science, 2013, 340, 491-495.	6.0	378

#	Article	IF	CITATIONS
127	CSPAD-140k: A versatile detector for LCLS experiments. Nuclear Instruments and Methods in Physics Research, Section A: Accelerators, Spectrometers, Detectors and Associated Equipment, 2013, 718, 550-553.	0.7	106
128	Femtosecond Visualization of Lattice Dynamics in Shock-Compressed Matter. Science, 2013, 342, 220-223.	6.0	176
129	Probing homogenous ice nucleation within supercooled bulk water droplet in "no man's land" with an ultrafast X-ray laser. , 2013, , .		0
130	Development, experimental performance and damage properties of x-ray optics for the LCLS free-electron laser. , 2013, , .		2
131	Ultra-precise characterization of LCLS hard X-ray focusing mirrors by high resolution slope measuring deflectometry. Optics Express, 2012, 20, 4525.	1.7	132
132	Energy-dispersive X-ray emission spectroscopy using an X-ray free-electron laser in a shot-by-shot mode. Proceedings of the National Academy of Sciences of the United States of America, 2012, 109, 19103-19107.	3.3	113
133	Nanoflow electrospinning serial femtosecond crystallography. Acta Crystallographica Section D: Biological Crystallography, 2012, 68, 1584-1587.	2.5	167
134	The CSPAD megapixel x-ray camera at LCLS. Proceedings of SPIE, 2012, , .	0.8	99
135	In vivo protein crystallization opens new routes in structural biology. Nature Methods, 2012, 9, 259-262.	9.0	193
136	Room temperature femtosecond X-ray diffraction of photosystem II microcrystals. Proceedings of the National Academy of Sciences of the United States of America, 2012, 109, 9721-9726.	3.3	144
137	High-Resolution Protein Structure Determination by Serial Femtosecond Crystallography. Science, 2012, 337, 362-364.	6.0	758
138	Lifetime and damage threshold properties of reflective x-ray coatings for the LCLS free-electron laser. Proceedings of SPIE, 2011, , .	0.8	7
139	Single mimivirus particles intercepted and imaged with an X-ray laser. Nature, 2011, 470, 78-81.	13.7	790
140	Femtosecond X-ray protein nanocrystallography. Nature, 2011, 470, 73-77.	13.7	1,771
141	A single-shot intensity-position monitor for hard x-ray FEL sources. Proceedings of SPIE, 2011, , .	0.8	34
142	Aerosol Imaging with a Soft X-Ray Free Electron Laser. Aerosol Science and Technology, 2010, 44, i-vi.	1.5	40
143	Femtosecond diffractive imaging of biological cells. Journal of Physics B: Atomic, Molecular and Optical Physics, 2010, 43, 194015.	0.6	41
144	The Coherent X-ray Imaging (CXI) instrument at the Linac Coherent Light Source (LCLS). New Journal of Physics, 2010, 12, 035024.	1.2	170

#	Article	IF	CITATIONS
145	Sacrificial Tamper Slows Down Sample Explosion in FLASH Diffraction Experiments. Physical Review Letters, 2010, 104, 064801.	2.9	59
146	Short-pulse Laser Induced Transient Structure Formation and Ablation Studied with Time-resolved Coherent XUV-scattering. Materials Research Society Symposia Proceedings, 2009, 1230, 1.	0.1	3
147	Coherent X-ray diffractive imaging of protein crystals. Journal of Synchrotron Radiation, 2008, 15, 576-583.	1.0	18
148	Ultrafast soft X-ray scattering and reference-enhanced diffractive imaging of weakly scattering nanoparticles. Journal of Electron Spectroscopy and Related Phenomena, 2008, 166-167, 65-73.	0.8	16
149	Ultrafast single-shot diffraction imaging of nanoscale dynamics. Nature Photonics, 2008, 2, 415-419.	15.6	221
150	Massively parallel X-ray holography. Nature Photonics, 2008, 2, 560-563.	15.6	168
151	Single Particle X-ray Diffractive Imaging. Nano Letters, 2008, 8, 310-316.	4.5	229
152	Non-destructive characterization and alignment of aerodynamically focused particle beams using single particle charge detection. Journal of Aerosol Science, 2008, 39, 917-928.	1.8	26
153	Camera for coherent diffractive imaging and holography with a soft-x-ray free-electron laser. Applied Optics, 2008, 47, 1673.	2.1	34
154	Femtosecond time-delay X-ray holography. Nature, 2007, 448, 676-679.	13.7	238
155	Radiation driven collapse of protein crystals. Journal of Synchrotron Radiation, 2006, 13, 1-7.	1.0	11
156	Femtosecond diffractive imaging with a soft-X-ray free-electron laser. Nature Physics, 2006, 2, 839-843.	6.5	910
157	Anomalous Two-Photon Compton Scattering. New Journal of Physics, 0, , .	1.2	1